ELSEVIER

Journal of Chemical Neuroanatomy 17 (2000) 183–197

Journal of CHEMICAL NEUROANATOMY

www.elsevier.com/locate/jchemneu

Constitutive and inducible nitric oxide synthases after dynorphin-induced spinal cord injury

Wen-Hui Hu [a,b,*], Wen-An Qiang [b], Fang Li [a], Na Liu [b], Guo-Qiang Wang [a], Hai-Yan Wang [a], Xuancai S.T. Wan [c], Wei-Hong Liao [a], Jing-Sheng Liu [b], Min-Feng Jen [b]

[a] *Department of Spinal Cord Injury, Research Institute of Surgery and Daping Hospital, The Third Military Medical University, Daping, Chongqing 400042, People's Republic of China*

[b] *Department of Pharmacology, Institute of Basic Medical Sciences, Peking Union Medical College and Chinese Academy of Medical Sciences, 5 Dong Dan San Tiao, Beijing 100005, People's Republic of China*

[c] *Department of Neurobiology, Institute of Basic Medical Sciences, Peking Union Medical College and Chinese Academy of Medical Sciences, 5 Dong Dan San Tiao, Beijing 100005, People's Republic of China*

Received 21 September 1998; received in revised form 15 March 1999; accepted 28 September 1999

Abstract

It has recently been demonstrated that selective inhibition of both neuronal constitutive and inducible nitric oxide synthases (ncNOS and iNOS) is neuroprotective in a model of dynorphin (Dyn) A(1–17)-induced spinal cord injury. In the present study, various methods including the conversion of ^{3}H-L-arginine to ^{3}H-citrulline, immunohistochemistry and in situ hybridization are employed to determine the temporal profiles of the enzymatic activities, immunoreactivities, and mRNA expression for both ncNOS and iNOS after intrathecal injection of a neurotoxic dose (20 nmol) of Dyn A(1–17). The expression of ncNOS immunoreactivity and mRNA increased as early as 30 min after injection and persisted for 1–4 h. At 24–48 h, the number of ncNOS positive cells remained elevated while most neurons died. The cNOS enzymatic activity in the ventral spinal cord also significantly increased at 30 min–48 h, but no significant changes in the dorsal spinal cord were observed. However, iNOS mRNA expression increased later at 2 h, iNOS immunoreactivity and enzymatic activity increased later at 4 h and persisted for 24–48 h after injection of 20 nmol Dyn A(1–17). These results indicate that both ncNOS and iNOS are associated with Dyn-induced spinal cord injury, with ncNOS predominantly involved at an early stage and iNOS at a later stage.

Keywords: Nitric oxide; Nitric oxide synthase; Dynorphin; Spinal cord injury; Neurotoxicity

1. Introduction

Nitric oxide (NO) is synthesized from L-arginine by NO synthase (NOS), an enzyme which exists in multiple isoforms in various species. In the central nervous system (CNS), two constitutive isoforms of NOS (cNOS) are expressed, one in neurons (ncNOS) and another in endothelial cells. An inducible isoform of NOS (iNOS) is expressed in a wide variety of cells, notably in macrophages or glia, after exposure to endotoxins or cytokines. The iNOS produces NO in large quantities independent of intracellular calcium.

NO production as well as NOS activity, immunoreactivity (IR), and mRNA expression are significantly increased in cerebral ischemia (Zhang et al., 1994; Iadecola et al., 1995a,b; Kuppusamy et al., 1995; Higuchi et al., 1996; Rao et al., 1998), experimental allergic encephalitis (Hooper et al., 1995; Van Dam et al., 1995), viral infection (Adamson et al., 1996; Meyding-Lamade et al., 1998; Haas et al., 1999; Li et al., 1999) and excitotoxic injuries (Schmidt et al., 1995; Lecanu et al., 1998; Perez-Severiano et al., 1998). Various injuries to the brain (Rao et al., 1998; Stojkovic et al., 1998; Wada et al., 1998, 1999) and spinal cord (Wu

* Corresponding author. Tel.: +86-23-6880-8963; fax: +86-23-6870-5094.

E-mail address: huwenhui98@hotmail.com (W.-H. Hu)

0891-0618/00/$ - see front matter
PII: S0891-0618(99)00039-3

et al., 1994; Hamada et al., 1996; Vizzard, 1997; Guizar-Sahagun et al., 1998; Winkler et al., 1998; Xu et al., 1998; Kaur et al., 1999) as well as axotomy (Herdegen et al., 1993; Rossiter et al., 1996; Nakagomi et al., 1999) also elevate NOS/NO expression. However, the implication of increased NOS/NO expression after CNS injury remains contentious. Various isoforms of NOS may play different roles in the double-edged effects of NO in CNS injury.

Dynorphin (Dyn) A(1–17), an endogenous kappa opioid ligand, induces transient or permanent paralysis of hindlimbs and tails upon intrathecal (i.t.) injection of high doses in normal rats (Faden, 1990; Long et al., 1994; Shukla and Lemaire, 1994; Tian et al., 1994), while its analgesic effects remain controversial (Hylden et al., 1991; Dubner and Ruda, 1992; Laughlin et al., 1997). After traumatic or inflammatory spinal cord injury (SCI), both the content of endogenous Dyn A(1–17) and the expression of prodynorphin mRNA are markedly increased in the spinal cord, implying that Dyn A(1–17) is implicated in SCI (Faden, 1990; Li et al., 1997; Tachibana et al., 1998). Activation of *N*-methyl-D-aspartate (NMDA) receptor is involved in the non-opioid neurotoxic effect of Dyn A(1–17) (Faden, 1990; Skilling et al., 1992; Long et al., 1994; Shukla and Lemaire, 1994; Chen et al., 1995). Since the calcium channel blocker verapamil prevents the spinal cord damage induced by Dyn, intracellular calcium may be involved in the damage (Chen et al., 1995). Among the intracellular events that are stimulated by calcium are the activation of NOS and the generation of NO. Therefore, Dyn A(1–17) may induce neurotoxicity through the NMDA-Ca^{2+}-NOS pathway. Our previous study with NADPH-diaphorase histochemistry suggested that Dyn spinal neurotoxicity induces NOS expression in the ventral horn cells (Hu et al., 1996).

Table 1
Definition for neurological scoring of hindlimbs in rats

Neuroscores	Functional definition
0	No spontaneous movement
1	No spontaneous movement but responds to hindlimb pinch
2	Spontaneous movement but unable to support weight (stand)
3	Stands but unable to walk
4	Walks on knuckles or on the medial surface of foot, lack of control of ankle or foot, uncoordinated gait
5	Walks, coordination of forelimbs and hindlimbs in gait, improved hindlimb postural support, abdomen not lowered to the ground, few toe drags
6	Walks, one or two toe drags, slight unsteadiness turning at full speed
7	Normal gait and body support, no loss of balance on fast turns, no toe drag

Recently, it has been demonstrated that selective inhibition of both ncNOS and iNOS is neuroprotective against Dyn-induced SCI (Hu et al., 1999). In the present study, various methods including enzyme assay, immunohistochemistry, and in situ hybridization histochemistry are employed to determine the time course of the enzyme activities, immunoreactivities, and mRNA expression of cNOS and iNOS after i.t. injection of a paralyzing dose of Dyn A(1–17). These results suggest that both ncNOS and iNOS are involved in Dyn-induced SCI, with ncNOS predominantly involved at an early stage and iNOS at a later stage.

2. Materials and methods

2.1. Animals and surgery

Wistar rats weighing 250–300 g were obtained from the Animal Breeding Center of the Chinese Academy of Medical Sciences. Rats were anesthetized with sodium pentobarbital. A self-made polyethylene catheter was inserted through a slit in the atlanto-occipital membrane and pushed 7.5 cm into the subarachnoid space around the rostral edge of the lumbar enlargement as described by Yaksh and Rudy (1976). The placement of the catheter tip at $L_{2\sim3}$ was confirmed at autopsy. All animals were allowed to recover for 24–36 h and only those rats with normal neurological function and no abnormal responses to i.t. saline injection were used for experiments. Ten microliters of Dyn A(1–17) (lot # 34523, Peninsula, Belmont, CA) or saline were infused and followed by 10 μl of saline to flush the catheter. Hindlimb neurological function was blindly evaluated by two investigators over a 48-h period after infusion.

2.2. Evaluation of hindlimb motor function

Neurological function was assessed by a combination of the 8-point ordinal scale described by Faden et al. (1987) and the open field walking scale described by Behrmann et al. (1993). The neuroscores were presented in Table 1.

2.3. cNOS and iNOS activity assay

Rats were killed by decapitation. Spinal cords between T_{11} and L_6 were quickly removed (within 20 s) onto an ice-cold paraffin plate. Under a dissection microscope, the spinal cord was drawn apart through the anterior median fissure and cut with a blade equally into dorsal and ventral parts. The dorsal and ventral parts were collected separately in Eppendorf tubes, briefly immersed in liquid nitrogen and stored at −70°C until the time of assay. The entire procedure from

decapitation to freezing required ~2 min and was maintained at 4°C.

NOS activity was measured as described previously (Qiang et al., 1996) by detecting the conversion of ^{3}H-L-arginine to ^{3}H-L-citrulline through a modification of the procedure described by Bredt and Snyder (1990) and Mayer et al. (1990). After being weighed, the sample was homogenized in 5 volumes of cold buffer A containing 50 mM HEPES, pH 7.4, 0.32 M sucrose, 1 mM EDTA, 0.1 mM EGTA, 1 mM phenylmethylsulfonal fluoride, 1 mM dithiothreitol and 1.5 mM 2-mercaptoethanol. The homogenate was centrifuged at 20 000 × *g* for 60 min at 4°C. The supernatant was tested in triplicate for assaying NOS activity and the precipitant for assaying ^{3}H-MK801 binding. The reaction buffer B contained 50 mM HEPES, pH 7.4, 1 mM β-NADPH, 30 μM 6(R)-5,6,7,8-tetrahydro-L-biopterin (BH_4), 10 nM calmodulin, 1.25 mM $CaCl_2$ and 1 mM EGTA. The reaction mixture containing 50 μl supernatant, 50 μl reaction buffer B and 0.2 μCi ^{3}H-L-arginine (100 000–150 000 cpm) was incubated at 37°C for 15 min. The reaction was stopped by adding 2 ml of ice-cold buffer C containing 20 mM HEPES, pH 5.5, 0.2 mM EGTA, 2 mM EDTA and 1 mM L-citrulline. The mixture was then applied to a 0.7–1.0 ml Dowex AG50WX8 (Na^+ form) anion-exchange column, and the unbound ^{3}H-L-citrulline was eluted with 2 ml of distilled water. The radioactivity in the eluate was measured by liquid scintillation counting (Beckman L9800). The enzymatic activity was expressed as pmol ^{3}H-L-citrulline per milligram protein per minute. Protein concentrations of the samples were measured with Bradford assay. The activity of iNOS was determined in the presence of 4 mM EGTA (a Ca^{2+}-chelating agent) and in the absence of calmodulin and $CaCl_2$ after subtracting the blank value, which represents the radioactivity in the presence of 1 mM N^{ω}-nitro-L-arginine methyl ester (L-NAME), a potent NOS inhibitor. The activity of cNOS was defined as the activity remaining after subtracting iNOS activity from the calcium-dependent total NOS activity (Salter et al., 1991). In preliminary studies, we measured the dose-response of various cofactors and substrates for NOS. The K_m for L-arginine was 1.6 μM. The EC_{50} for calcium, calmodulin, β-NADPH and BH_4 were 0.55, 1.33, 32.5 and 0.43 μM, respectively. Addition of ~3–5 mM EGTA completely abolished all NOS activity. Both trifluoperazine, a calmodulin antagonist, and L-NAME inhibited NOS activity at a 1 mM concentration with IC_{50} value of 12.7 and 1.56 μM, respectively, in this assay.

2.4. Perfusion and tissue processing

Animals were perfused under deep anesthesia with sodium pentobarbital (50 mg/kg, i.p.) via the ascending aorta with 200 ml of autoclaved 0.1 M phosphate buffered saline (PBS) followed by 400 ml of ice-cold 4% paraformaldehyde in 0.1 M PBS. The spinal segment 2 cm rostral and caudal to the tip of the implanted catheter was dissected and post-fixed for 2–3 h in the same fixative at 4°C, and then cryoprotected overnight with 20% sucrose at 4°C.

Blocks of 0.5-cm segments of spinal cord above and below from the i.t. catheter tip were cut transversally, and some of them were labeled longitudinally by unilateral or bilateral incision. For comparison, the labeled and unlabeled segmental cords were sectioned together on a sliding microtome. Five 1-in-5 series of 40-μm-thick frozen sections were collected in sterile Eppendorf tubes containing 20% sucrose in 0.1 M PBS and stored at −20°C until use. One set of sections was stained with thionin, and the others were used for immunohistochemistry and in situ hybridization histochemistry.

2.5. Immunocytochemistry

After rinsing thoroughly with 0.01 M PBS, the free-floating spinal sections were incubated in 10% normal goat serum for 30 min and then with primary antibody in 0.01 M PBS containing 1% normal goat serum and 1% Triton X-100 at 4°C for 24 h. The affinity purified polyclonal antibody to rat ncNOS was a generous gift from Dr Ted M. Dawson (Johns Hopkins University School of Medicine), and the rabbit polyclonal antibody to mouse iNOS (sc-650) was purchased from Santa Cruz (California, CA). The sections were then washed in 0.01 M PBS, and the staining procedure was performed according to the specifications of the manufacturer (Histostain-SP kit, Zymed Laboratories, South San Francisco, CA) using diaminobenzidine hydrochloride (Sigma, St. Louis, MO) as the chromogen. Sections were mounted on gelatin-coated slides, air-dried, dehydrated, cleared in xylene and coverslipped. Positive staining was abolished upon omission of the primary or secondary antibody. To reduce variability in the processing, sections from both experimental and control groups were processed simultaneously using the same reagents in the same staining tube. All sections were processed in parallel to allow comparison between different experimental groups.

2.6. In situ hybridization histochemistry

The chosen cDNA probes were labeled with digoxigenin (DIG)-dUTP and quantified according to the protocol of the commercial kit (Boehringer-Mannheim, Germany). Free-floating sections were pretreated with 0.1 M PBS, 0.4% Triton X-100 in PBS, 10 μg/ml proteinase, K, 4% ice-cold paraformalde-

hyde, 0.2 N HCl and 2 × salt sodium citrate (SSC). Prehybidization of the sections was then carried out for 2 h at 42–45°C in the prehybridization solution containing 50% deionized formamide, 5 × SSC, 10% dextran sulphate, 0.5% sodium dodecyl sulfate (SDS), 200 μg/ml heat-denatured and sheared salmon sperm DNA and 2 × Den'hardt. The hybridization solution was prepared by adding the DIG-labeled cDNA probe to a final concentration of 0.5 ng/μl in the prehybridization solution and heat-denatured each time before use. About 30–60 μl of hybridization solution was added into each Eppendorf tube and the hybridization was carried out at 42–45°C for 20 h. After washing with pre-warmed 2 × SSC/50% formamide at 42–45°C for 2 × 15 min followed by 0.1 × SSC/50% formamide and 0.1 × SSC at 42–45°C for 15 min each, the sections were immunohistochemically stained with alkaline phosphatase labeled anti-DIG Fab fragment according to the protocol of the commercial kit (Boehringer-Mannheim, Germany). The color reaction was carefully monitored until sufficient reaction product had developed in the cells of interest and then stopped by rinsing the sections in distilled water. The sections were finally mounted on gelatin-coated slides, air-dried and directly cleared in xylene and coverslipped. Hybridization in the absence of the DIG-labeled probe or anti-DIG antibody and pretreatment of the sections with 100 μg/ml RNAse at 37°C were employed for controls. All sections were processed in parallel to allow for comparison between different groups and different probes.

2.7. Microscopic observations and cell counting

The individual laminae and segmental levels of thoraco-lumbar spinal cords were determined based on the schematic cytoarchitecture described by Molander et al. (1984). For ncNOS-IR, the number of positive cells in the individual spinal cord laminae was counted blindly by two investigators (Hu W.H. and Li F.) in 20–30 1-in-5 sequential sections per animal using a 20 × objective and bright illustration. The number of positive cells on the left and right side of the spinal cord was combined for statistical analysis since no significant difference was observed.

2.8. Statistical analysis

Neurological ordinal scores were compared using Kruskal–Wallis ANOVA and Mann–Whitney *U* tests. Differences of NOS activities and ncNOS-IR between experimental and control groups were compared by ANOVA and Newman–Keuls test and post-hoc unpaired *t*-tests. Data are expressed as mean ± standard deviation (S.D.).

3. Results

3.1. Dyn neurotoxicity in rat spinal cord

It is well-known that i.t. injection of Dyn A(1–17) produces dose-dependent paralysis of hindlimbs and tails in rats (Faden, 1990; Long et al., 1994; Shukla and Lemaire, 1994; Tian et al., 1994). However, the neurotoxic doses of Dyn A(1–17) have varied. In the present study, 5 nmol Dyn A(1–17) produced transient paralysis in six out of eight rats with full recovery within 1 h. After i.t. injection of 10 nmol Dyn A(1–17), five out of 11 rats underwent transient paralysis with almost complete recovery within 1 h. Two rats developed permanent paraplegia with no recovery within 24 h. Fifteen nmol Dyn A(1–17) induced transient paralysis in one out of seven rats and permanent paraplegia in four out of seven rats. At 20 nmol, all 19 rats were severely paralyzed. One showed full recovery of motor function within 1 h and 2 within 4 h, but the remainder had no trace of neurological recovery (Fig. 1). Hindlimb paralysis usually concurred with paralysis of the tail, especially at higher dosages of Dyn A(1–17). Tails showed earlier paralysis and later functional recovery than the hindlimbs. Occasionally, only tail paralysis occurred in some rats. Hindlimb paralysis, however, never occurred without tail paralysis. This phenomenon supports the hypothesis that Dyn-induced spinal analgesia remains indefinite due to loss of tail flick (Hylden et al., 1991; Dubner and Ruda, 1992; Laughlin et al., 1997).

The histopathological changes of the spinal cord after i.t. injection of Dyn A(1–17) were described previously (Tian et al., 1994; Hu et al., 1996). Generally, 20 nmol Dyn A(1–17) produced progressive and irreversible neuronal death and gliosis, maximizing at the tip of the i.t. catheter and centering on the central gray matter. In the most seriously damaged cases, the entire gray matter and its surrounding white matter were intensely necrotic and lost during the staining process, leaving behind a small peripheral rim of white matter and superficial dorsal horn. It was most remarkable 0.5 cm from the tip of the i.t. catheter.

3.2. Temporal profile of cNOS and iNOS activities in ventral and dorsal spinal cord

Since the dorsal and ventral regions of the spinal cord have quite different functional morphologies, the spinal cords were carefully dissected into dorsal and ventral parts. In saline-injected control rats, the cNOS activity assayed by the conversion of ^{3}H-L-Arg into ^{3}H-L-citrulline was significantly higher in the dorsal than in the ventral regions. However, there was no significant difference in iNOS activity between the dorsal and the ventral regions. The cNOS activity was significantly higher than the iNOS activity both in the

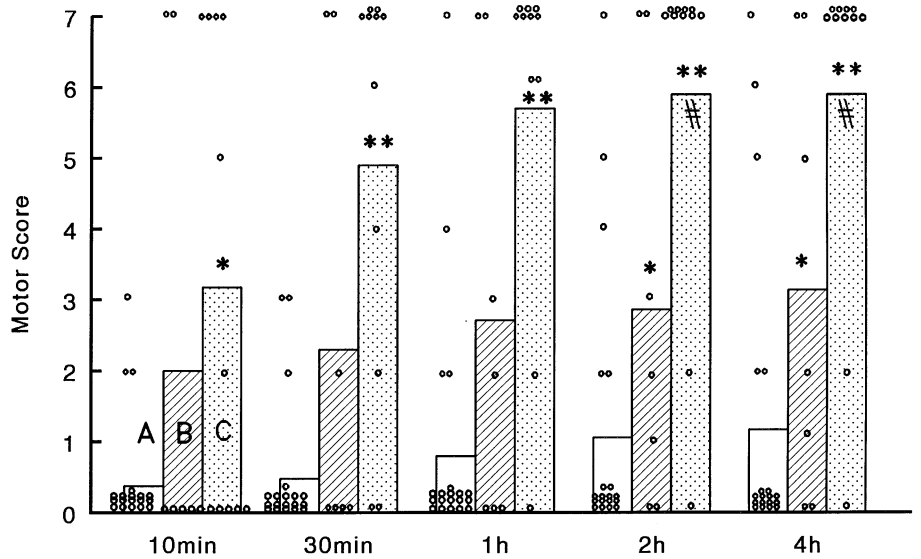

Fig. 1. Dose-response effect of intrathecal (i.t.) injection of dynorphin (Dyn) A(1–17) on rat hindlimb motor function. (A) 20 nmol, (B) 15 nmol and (C) 10 nmol Dyn A(1–17). * $P < 0.05$, ** $P < 0.01$ and # $P < 0.05$ indicate statistical significance as compared with A and B respectively by Mann–Whitney U test. Dots represent the number of animals.

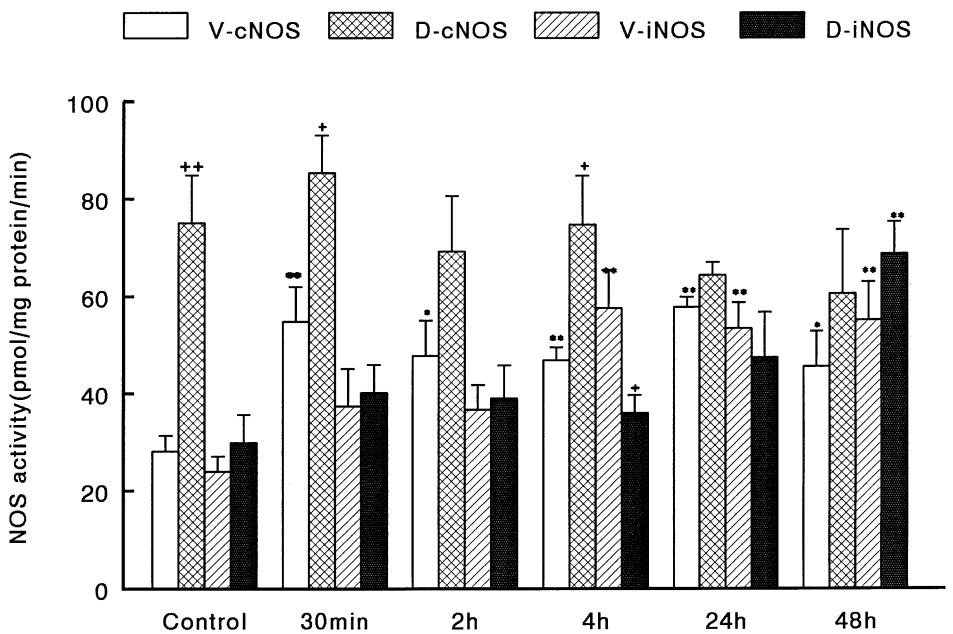

Fig. 2. Activities of constitutive and inducible nitric oxide synthases (cNOS and iNOS) in the supernatant of the ventral (V) and dorsal (D) spinal cord after 20 nmol dynorphin (Dyn) A(1–17)-induced spinal neurotoxicity. V-cNOS significantly increased at 30 min but V-iNOS increased at 4 h. * $P < 0.05$. ** $P < 0.01$ and + $P < 0.05$. + + $P < 0.01$ indicate statistical significance as compared with the corresponding saline control and the ventral spinal cord respectively.

dissected dorsal cord and in the entire non-dissected cord, while no significant difference between cNOS and iNOS activities was observed in the ventral spinal cord (Fig. 2 and see below). The presence of cNOS activity in the control rats is comprehensible, but it is unclear why iNOS activity is also present in control rats (Iadecola et al., 1995b; Schmidt et al., 1995). It is possible that the control rats were not normal since they were also sham-operated. It is also possible that removal of Ca^{2+} and calmodulin during bioassay may not have completely blocked the conversion of L-arginine into L-citrulline.

There were no significant differences in the activities of cNOS and iNOS among the saline control rats at various time points. At 30 min–48 h after i.t. injection of 20 nmol Dyn A(1–17), the cNOS activity significantly increased in the ventral cord compared to the control, but no significant change in the dorsal cord

was observed. The iNOS activity in the ventral cord showed no significant change at 30 min–2 h after i.t. injection of 20 nmol Dyn A(1–17), but they increased at 4 h and persisted up to 24–48 h. The iNOS activity in the dorsal cord also increased significantly ($P < 0.01$) 48 h after i.t. injection of 20 nmol Dyn A(1–17) (Fig. 2). Similar trends were observed in the cNOS and iNOS activities in the entire segment of the non-dissected spinal cord. The cNOS activity in the entire spinal cord significantly increased from 28.47 ± 3.33 ($n = 5$) in the controls to 38.97 ± 3.94 ($n = 7$, $P < 0.05$) and 54.04 ± 1.74 pmol/mg per min ($n = 5$, $P < 0.01$) 2 and 24 h, respectively, after injection. The iNOS activity of control rats was 16.83 ± 2.70 pmol/mg per min ($n = 5$), 19.73 ± 1.47 ($n = 7$, $P > 0.05$) after 2 h but significantly increased to 27.69 ± 4.24 ($n = 5$, $P < 0.05$) after 24 h.

3.3. ncNOS and iNOS immunoreactivities in normal and injured spinal cord

In control rats, ncNOS-IR neurons and fibers were located mainly in laminae I–II and X as well as in the intermediolateral cell column (IML). A few isolated and slight-stained neurons with long processes were occasionally observed in laminae VII, VIII and IX. Large motoneurons in laminae VIII and IX and the lateral and medial group (LG, MG) in lamina VII were negative. These staining patterns are consistent with previous reports (Dun et al., 1993; Vizzard et al., 1994).

As early as 5–30 min after i.t. injection of 20 nmol Dyn A(1–17), ncNOS-IR expression was dramatically enhanced. It peaked at 1–2 h and remained elevated at 3–4 h (Table 2, Fig. 3). The number of ncNOS-IR-positive cells and their intensities in lamina X and IML significantly increased. The staining for ncNOS-IR in lamina I–II also slightly increased. In laminae VII, VIII and IX, a number of neurons stained strongly for ncNOS-IR. These neurons with extensive processes were mainly distributed in the LG and MG of lamina VII and in a few motoneurons. However, not all of the motoneurons and interneurons were positively stained. Staining for ncNOS-IR was most abundant in L_2–L_3, depending upon the severity and site of the pathological abnormality. At 24 and 48 h, although most neurons were dead, a number of ncNOS-IR positive cells remained significantly elevated (Table 2, Fig. 4). Since some of the cells in the spinal sections showing severe necrosis might have been lost during the staining procedure, the relative percentage of ncNOS-IR neurons at 48 h may be misleading. However, abundant staining for ncNOS-IR was observed in the 3rd and 4th segments of the spinal cord at 24–48 h, which displayed less pathological damage (Fig. 4E,F). Furthermore, in some spinal sections with asymmetrical damage, more ncNOS-positive neurons were present on the slight-damaged side than on the side exhibiting severe necrosis (Fig. 4A). Most of the surviving neurons with intact morphology in the necrotic penumbra were strongly stained for ncNOS-IR (Fig. 4A–D). This selective resistance of ncNOS-positive neurons to CNS injury has been widely reported (Hyman et al., 1992; Mufson and Brandabur, 1994; Zhang et al., 1994; Behrens et al., 1996; Marsala et al., 1997; Gonzalez-Zulueta et al., 1998; Bishop et al., 1999).

The ncNOS-IR staining was absent in all glial, ependymal, and microvascular cells. However, the spinal pial arteries were stained positively for ncNOS-IR in both the control and experimental rats (Fig. 3A and Fig. 4A,B). This finding is supported by previous reports that ncNOS could not be found in parenchymal microvasculature but is present only in pial vessels of the brain and spinal cord (Catalan et al., 1996; Seidel et al., 1997).

Table 2
Quantitative counting for number of neuronal constitutive nitric oxide synthase (ncNOS)-immunoreactivity (IR)-positive cells in spinal cords after dynorphin-induced spinal cord injury[a]

	Spinal cord laminae				
	I–III	IV–VI	VII–IX	X	IML
Control (36)	34 ± 14	17 ± 10	11 ± 9	12 ± 5	5 ± 3
Dyn 30 min (27)	52 ± 20***	26 ± 11*	27 ± 11***	22 ± 6***	11 ± 7**
Dyn 2 h (45)	52 ± 19***	25 ± 11**	25 ± 12***	21 ± 8***	8 ± 4*
Dyn 4 h (39)	51 ± 22***	21 ± 9	16 ± 13	18 ± 9***	11 ± 6**
Dyn 48 h (55)	42 ± 13*	20 ± 10	23 ± 14***	15 ± 9***	13 ± 4***

[a] Number in parentheses represents 1-in-5 sections of spinal cord.
* $P < 0.05$;
** $P < 0.01$;
*** $P < 0.001$ indicate statistical significance as compared with saline control.

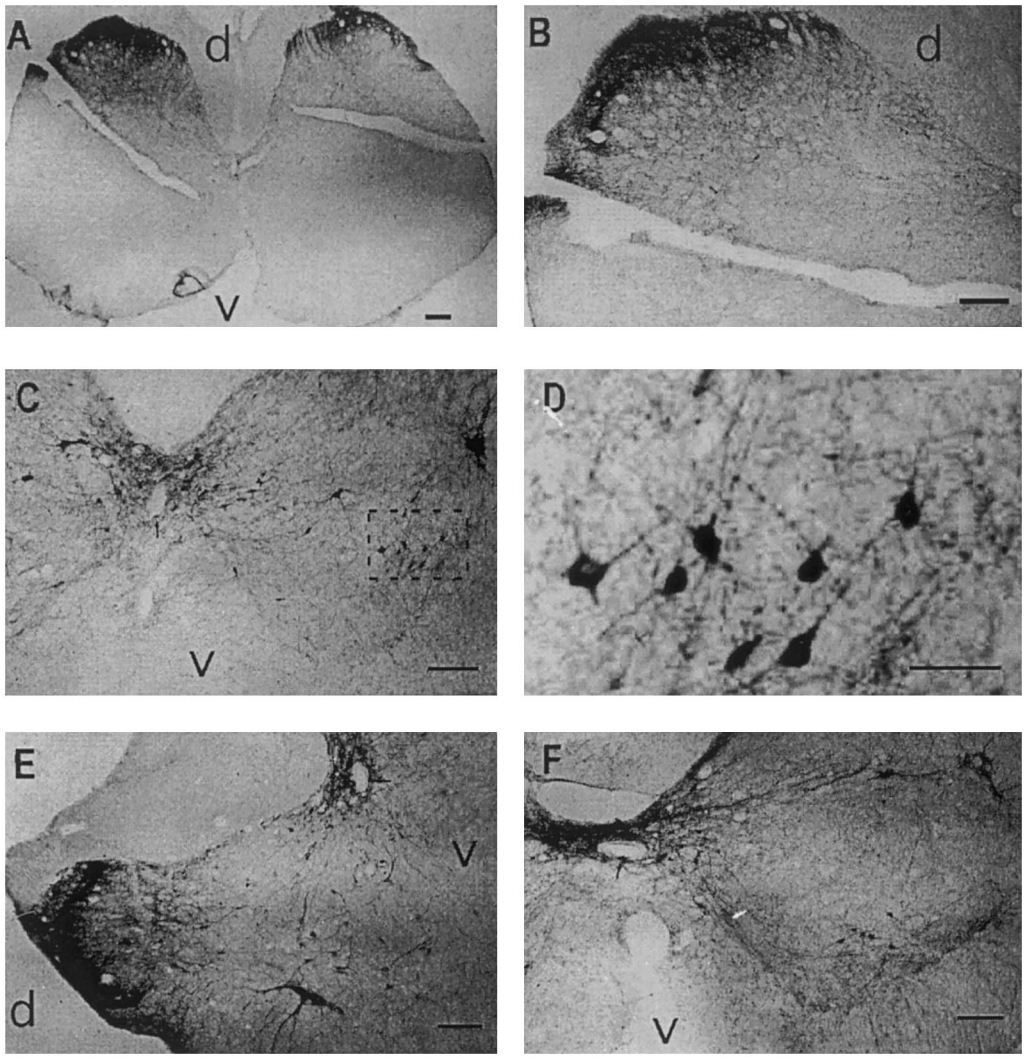

Fig. 3. Neuronal constitutive nitric oxide synthases (ncNOS) immunohistochemistry for the first segment of spinal cord from the intrathecal (i.t.) catheter tip in rats of the saline-injected control group (A and B) and the experimental groups at 1 h (C and D), 2 h (E), and 4 h (F) after i.t. injection of 20 nmol dynorphin (Dyn) A(1–17). The positive cells and fibers were distributed mainly in laminae I–II and X in the saline control. After i.t. injection of Dyn A(1–17), the number of positive neurons in laminae I–II increased (E) in comparison with a saline-injected control (B), making the laminar structure more visible. In laminae X and intermediolateral cell column (IML), more neurons and fibers stained positively and the ventral longitudinal fasciculus was also positive (small arrow). In the ventral horn, especially laminae VII, many scattered and medium-sized neurons were intensely positive with abundant and long beaded processes. However, most large motoneurons were negative. A few neurons also stained positively in the deeper dorsal horn (laminae IV–VI). (B) magnification of the left dorsal horn of (A). (D) magnification of (C). d and v indicate the dorsal and ventral orientation of the spinal cord. The lateral incision (A,B) is for labeling to distinguish the control and experimental sections of spinal cord stained in one tube. Scale bars = 100 μm.

No iNOS-IR-positive cells were observed in the spinal cords in the saline-injected controls and at 1–3 h after i.t. injection of 20 nmol Dyn A(1–17). However, iNOS-IR-positive cells were visible at 4–48 h after injection. They were mainly located around the edge of the peripheral white matter. At 48 h, many iNOS-IR-positive cells were present around and within the necrotic region of the spinal cord (Fig. 5). The positive cells appeared to resemble glial cells or epithelial cells in location and size, although neurons could not be excluded. Immunohistochemical multiple labeling for identifying the cell types deserves further study.

3.4. Expression of ncNOS and iNOS mRNA

To ensure the probe specificities for ncNOS and iNOS, the DNA sequences and restriction enzyme sites were analyzed. Digestion of ncNOS cDNA plasmid (from Dr Ted M. Dawson) and iNOS cDNA plasmid (from Dr Charles J. Lowenstein) with Acc I generated two exclusive fragments of 592 (564 plus 28) and 684 bp

(4018 – 3334), respectively. Both shared no homology to other isoforms of NOS and no cross-reactivity between ncNOS and iNOS in the plasmid dot hybridization (data not shown). However, the fragments of Bam HI-digested 2811 bp and Hind III-digested 997 bp for ncNOS cDNA shared 45 and 68% homology with iNOS, respectively, while the fragments of Bam HI 800 bp and Eco RI 990 bp for iNOS cDNA shared 42 and 48% homology with ncNOS, respectively. These fragments exhibited varying degrees of cross-reactivity between ncNOS and iNOS in the plasmid dot hybridization. To further confirm the probe specificity, i.t. injection of lipopolysaccharide (LPS) 20 μg/10 μl was performed. The LPS stimulation induced extensive and typical expression of iNOS mRNA in the spinal cord as detected with the 684 bp probe but did not induce ncNOS mRNA expression as detected with the 592 bp probe. These results were compatible with results obtained by in situ hybridization in spinal cord sections from the saline control and experimental rats. Finally, in situ hybridization and post-hybridization washes were performed under high stringent conditions.

In the control rats, ncNOS mRNA was most abundant in laminae I–II, and lamina X. Slight to moderate expression of ncNOS mRNA was also found in motoneurons of the spinal ventral horn. After i.t. injection of 20 nmol Dyn A(1–17), ncNOS mRNA appeared as early as 5–30 min and increased progressively for 1–4 h

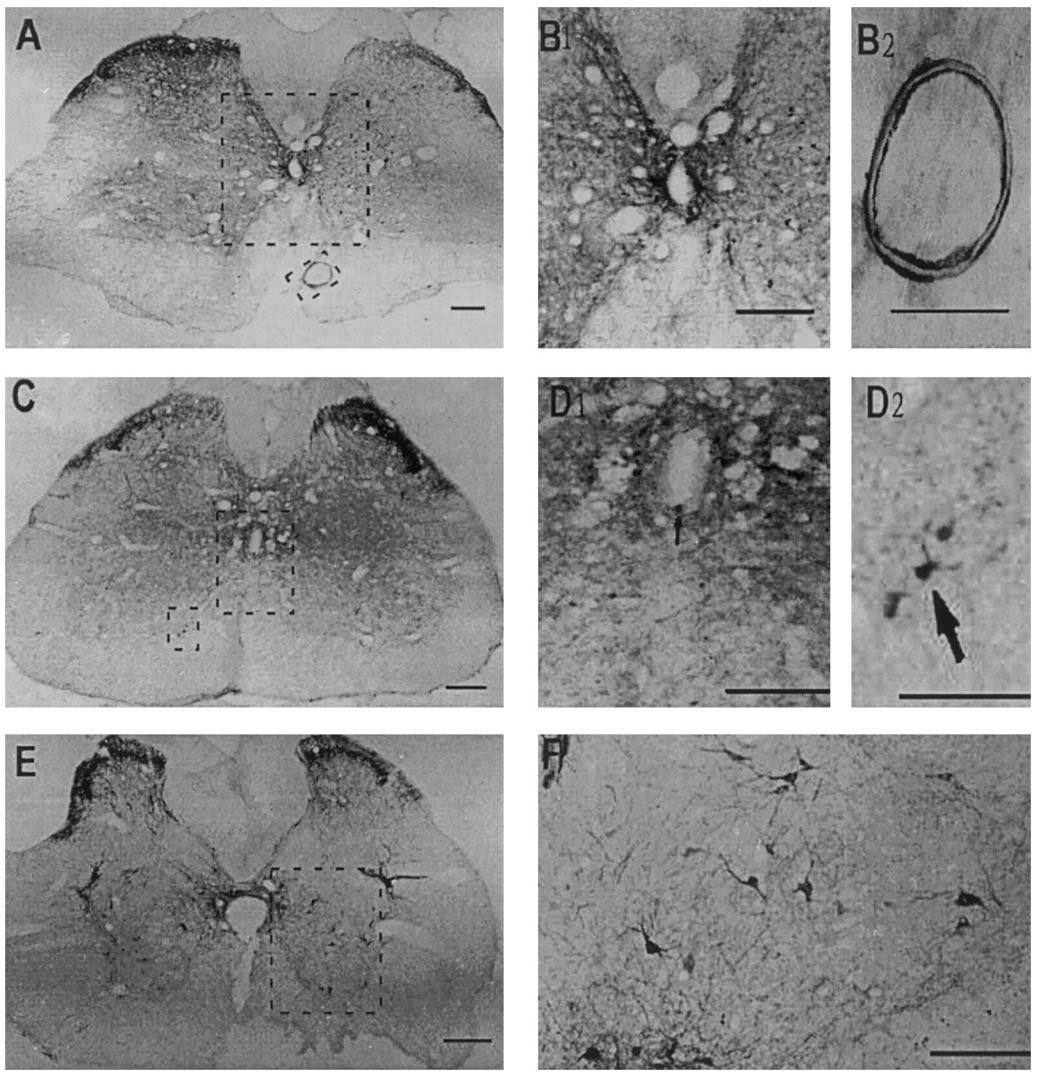

Fig. 4. Neuronal constitutive nitric oxide synthases (ncNOS) immunohistochemistry of rat lumbar spinal sections 24 h (A, B) and 48 h (C–F) after intrathecal (i.t.) injection of 20 nmol dynorphin (Dyn) A(1–17). Central necrosis was marked and more severe on one side of some spinal sections (A). Note the intact morphological structure of laminae X and dorsal horn with a number of ncNOS-positive neurons (A, B_1, C, D_1) and a few intensely-stained neurons (large arrow) at the border of necrosis (C_1, D_1). Extensive distribution and intense staining of ncNOS-positive neurons were observed in the fourth segment of spinal cord from the i.t. catheter tip (E, F). The intimal and adventitial tunicae of the anterior media spinal artery were intensely positive (A, B_2) but the parenchymal microvasculature was negative. (B, D, F) are magnified from (A), (C) and (E), respectively. Scale bars = 100 μm.

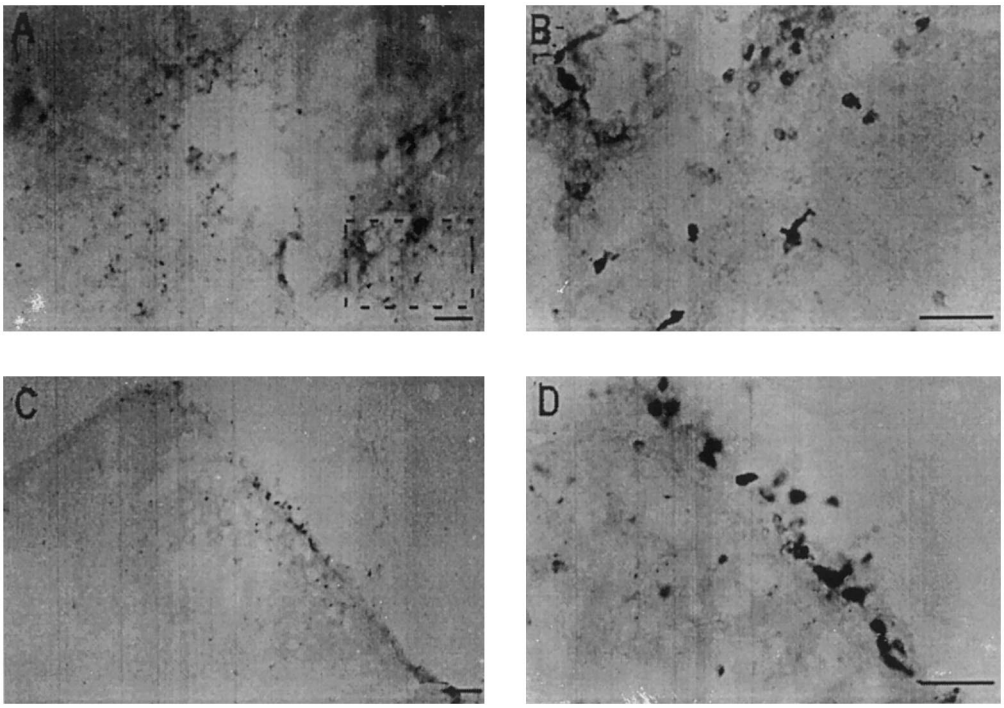

Fig. 5. Inducible nitric oxide synthases (iNOS) immunohistochemistry of rat lumbar spinal sections 48 h after intrathecal (i.t.) injection of 20 nmol dynorphin (Dyn) A(1–17). (A, B) shows the iNOS-immunoreactivity (IR)-positive cells within the necrotic zone of the central gray matter of the spinal cord. (C, D) display the strong iNOS-IR-positive cells around the margin of dorsal white matter. (B, D) are magnified from (A) and (C), respectively. Scale bars = 100 μm.

(Fig. 6). Expression was highest in large motoneurons of laminae VIII and IX and the dorsal nucleus (Clark column) and less in the medium- and small-sized neurons in the lateral and ventral horns. Some neurons in the deeper layer of the dorsal horn (Laminae IV and V) also expressed ncNOS mRNA. At 24–48 h, surviving motoneurons and interneurons retained their ncNOS mRNA expression and an intact morphological integrity, but ncNOS mRNA was absent in glial, ependymal, and microvascular endothelial cells, both in the control and experimental groups.

In contrast, typical signals for iNOS mRNA in control rats were moderately detected in large motoneurons of the ventral horn, dorsal nucleus, and in ependymal cells, but rarely in glial cells and small neurons (Fig. 7A). After i.t. injection of 20 nmol Dyn A(1–17), iNOS mRNA expression did not change significantly between 5 min and 1 h, but rose at 2–3 h and peaked at 4 h. Expression was greatest in large motoneurons, dorsal nucleus, lamina VII and ependymal cells. Glial cells (especially in white matter) also expressed iNOS mRNA at 2–4 h (Fig. 7B–D). The expression of iNOS mRNA remained high 24 and 48 h after i.t. injection of 20 nmol Dyn A(1–17), predominantly in glial cells and/or small neurons (both in gray and white matter) since most motoneurons had already died by this time. In those lumbar spinal sections with marked central necrosis, a few cells (most likely glial cells) expressing iNOS mRNA were found within the necrotic area. Surviving motoneurons and small neurons with positive signals were scattered in the penumbra (Fig. 7E–H).

4. Discussion

It is generally accepted that Dyn is neurotoxic upon intrathecal injection. However, the mechanisms responsible for Dyn-induced SCI are unknown. Both local ischemia (Long et al., 1994) and direct cytotoxicity have been implicated. Previous studies (Tian et al., 1994; Chen et al., 1995) together with other reports (Faden, 1990; Shukla and Lemaire, 1994) have indicated that the direct neurotoxicity of Dyn A(1–17) at the cellular level may involve both opioid and non-opioid effects. Pharmacological blockade with various competitive and non-competitive NMDA receptor antagonists prevents Dyn-induced motor dysfunction in rats (Faden, 1990; Long et al., 1994; Chen et al., 1995). Dyn A(1–17) increases the concentrations of glutamate and aspartate in the cerebrospinal fluid and particularly in the extracellular fluid of the spinal cord (Skilling et al., 1992). Dyn also enhances high potassium-induced glutamate release in rat spinal slices (Li et al., 1997). Receptor binding studies using rat brain membranes have demonstrated that Dyn interacts directly with NMDA receptors at the glutamate, glycine, and phencyclidine

sites (Dumont and Lemaire, 1994; Shukla and Lemaire, 1994). It has been reported that high concentrations of Dyn A(1–17) induce a sustained and irreversible overload of intracellular free calcium in cultured rat single spinal neurons via both NMDA and kappa opioid receptor activation (Hu et al., 1998). Among the intracellular events that are stimulated by calcium are the activation of NOS and the generation of NO. A considerable body of evidence exists to demonstrate that NO may be neurodestructive both in vitro and in vivo by generating toxic free radicals, inducing genotoxicity, activating poly (ADP-ribose) synthetase, and enhancing glutamate release. Therefore, Dyn may produce spinal neurotoxicity through the NMDA-Ca^{2+}-NOS/NO pathway. Using NADPH-diaphorase staining, a relatively specific histochemical marker for NOS, it was reported that Dyn does induce NOS expression in the ventral horn cells (Hu et al., 1996). Using selective ncNOS and iNOS inhibitors (7-nitroindazole and aminoguanidine), we reported that both ncNOS and iNOS are involved in Dyn-induced SCI (Hu et al., 1999). In the present study, we further demonstrate that enzymatic activities and mRNA expression of both ncNOS and iNOS increased in the ventral spinal cord after Dyn-induced spinal neurotoxicity. This finding is consistent with previous demonstrations that both ncNOS and iNOS contribute to the pathophysiological processes in other models of CNS injury such as ischemia, trauma, excitotoxicity and neurodegenerative diseases (for reviews, see Dalkara and Moskowitz, 1994; Iadecola, 1997; Parkinson et al., 1997; McCann et al., 1998; Strijbos, 1998; Bolanos and Almeida, 1999; Callsen-Cencic et al., 1999).

It has been documented that both iNOS mRNA and iNOS protein in the CNS do not change until 2–4 h after systemic LPS treatment (Liu et al., 1993; Iadecola et al., 1995a; Harada et al., 1999). After cerebral ischemia, expression of iNOS mRNA begins to increase at 12 h, but iNOS activity and immunoreactivity are not elevated until 2 days (Iadecola et al., 1995a,b). After traumatic injuries of the brain (Wada et al., 1998) or spinal cord (Bethea et al., 1998), iNOS activity is not increased, and iNOS immunoreactivity is not detected until 3 days. iNOS activity is significantly increased 2 days after NMDA-induced lesions in the striatum (Lecanu et al., 1998). However, RT-PCR reveals that the iNOS mRNA rises at 6 h and peaks at 24 h after an intrastriatal ethanol injection (Takeuchi et al., 1998) or after cortical cryogenic lesions (Knerlich et al., 1999). The relatively selective iNOS inhibitor aminoguanidine reduces cerebral infarct volume even when administrated 24 h after the middle cerebral artery is occluded either transiently (Zhang et al., 1996) or permanently (Iadecola et al., 1995b). The present study demonstrates that a few hours are needed for iNOS to be induced after Dyn-induced neurotoxicity. Later expression of iNOS may reveal a local inflammatory response after CNS injury (Licinio et al., 1999). Dyn and kappa

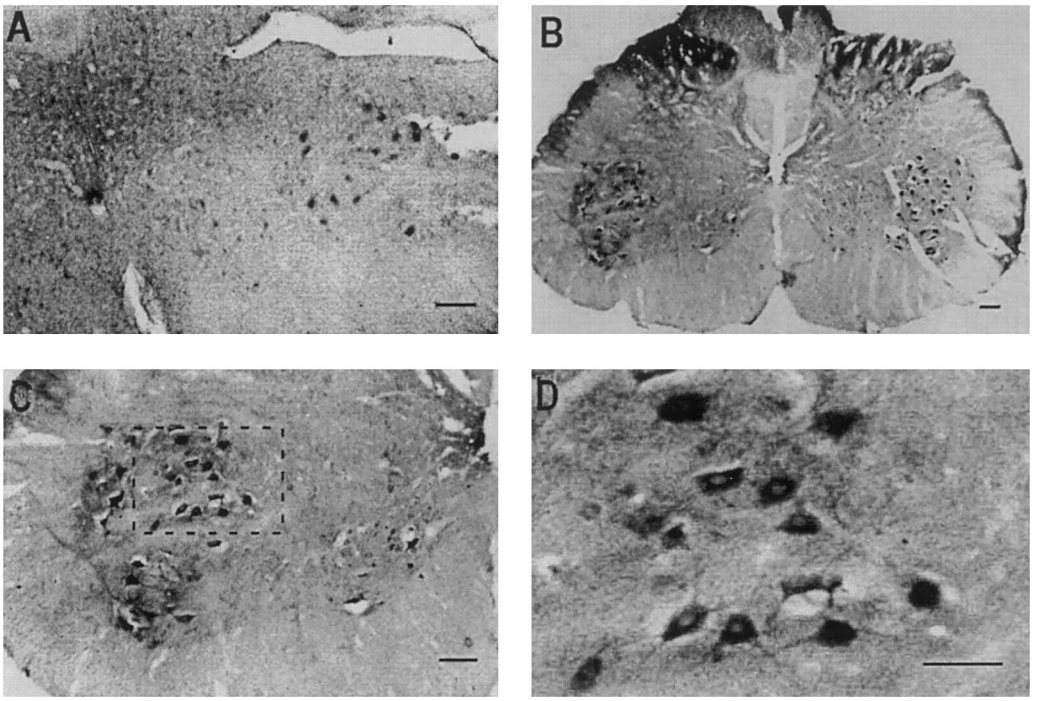

Fig. 6. In situ hybridization with neuronal constitutive nitric oxide synthases (ncNOS) for the first segment of spinal cord from the intrathecal (i.t.) catheter tip in saline-injected control rats (A) and experimental rats (B–D) 4 h after i.t. injection of 20 nmol dynorphin (Dyn) A(1–17). Dyn A(1–17) induced extensive mRNA expression of ncNOS with typical signals in motoneurons. (C) is the left ventral horn of the spinal cord in (B). (D) is further magnified from (C). Scale bars = 100 μm.

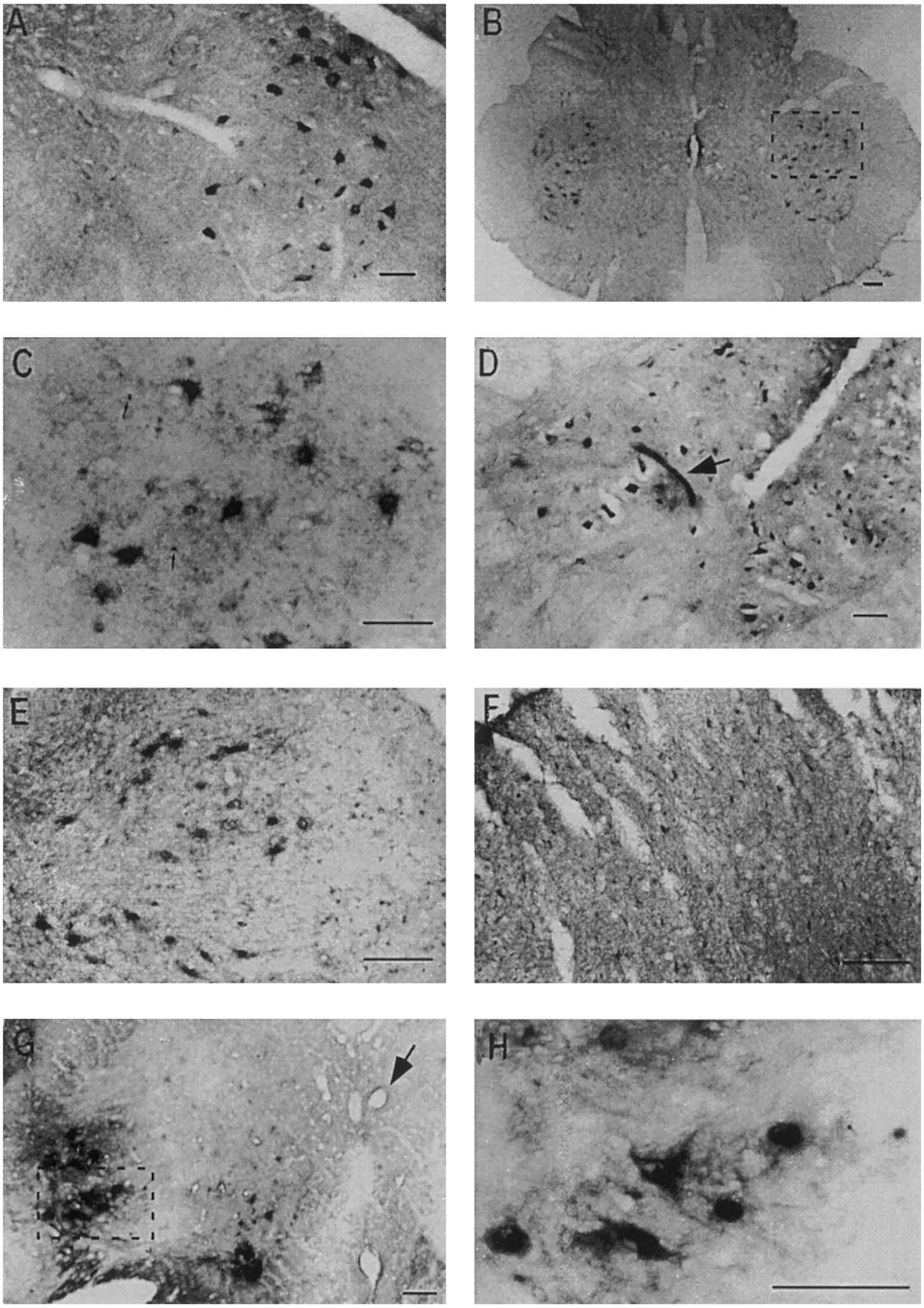

Fig. 7. In situ hybridization with inducible nitric oxide synthases (iNOS) for the first segment of spinal cord from the intrathecal (i.t.) catheter tip in saline-injected control rats (A) and experimental rats 2 h (B, C), 4 h (D), 24 h (E, F) and 48 h (G, H) after i.t. injection of 20 nmol dynorphin (Dyn) A(1–17). Typical signals were moderately detected in motoneurons of saline-injected control rats. Dyn A(1–17) induced intensive expression in motoneurons, interneurons, glial cells (in white matter especially, small arrow, C and F), ependymal cells (B) and the microvascular wall (D, G, middle arrow). (C, H) are magnified from (B, G), respectively (dashed square). (F) is the white matter of another spinal section. (B) shows the whole spinal cord. (A, E) are from the ventral horn of spinal cord. Scale bars = 100 μm.

opioid receptor have been reported to be involved in the inflammatory process (Hassan et al., 1992; Herz, 1996; Sheng et al., 1997). The correlation of inflammatory cytokines, such as tumor necrosis factor (TNF) family members, with Dyn-induced SCI deserves further study.

In the CNS, neurons express only cNOS, activated microglial cells and vascular smooth muscle cells ex-

press only iNOS, while astrocytes and endothelial cells express both cNOS and iNOS (Murphy et al., 1993). The present study further demonstrates that the expression of ncNOS-IR and its mRNA is restricted in neurons of both normal and injured spinal cords. Although ncNOS-IR is occasionally found in the endothelium of small spinal arteries, vascular smooth muscle cells do not express ncNOS (Catalan et al., 1996; Seidel et al., 1997).

The cellular sources of iNOS after in vivo CNS injury remain controversial. Earlier studies demonstrated that a hippocampal lesion (Wallace and Fredens, 1992) and transient global ischemia (Endoh et al., 1993) induce astrocytes to express NADPH-diaphorase activity. However, in some studies, only polymorphonuclear cells in the infarct penumbra after focal ischemia were iNOS-IR-positive. Macrophages, astrocytes and smooth muscle cells were all iNOS-IR-negative (Iadecola et al., 1995b; Coeroli et al., 1998). With the demyelinating multiple sclerosis-like lesion (De Groot et al., 1997) or with cortical incision (Yamanaka et al., 1998), strong iNOS-IR staining is found exclusively in perivascular and parenchymal macrophages. Injuries to the striatum (Takeuchi et al., 1998), hippocampus (Stojkovic et al., 1998) and cortex (Knerlich et al., 1999) induce reactive microglial expression of iNOS. After traumatic brain injury, the major cellular sources of iNOS expression are astrocytes and macrophages (Wada et al., 1998, 1999). In traumatic SCI (Bethea et al., 1998), iNOS coexpression with NF-kappaB in neurons and macrophages/microglia but not astrocytes is visible. The present study is the first report to demonstrate iNOS expression in glial cells and neurons in Dyn-induced SCI. The subtype of glial cells expressing iNOS has not been identified.

The observation of iNOS expression in (moto)neurons is consistent with previous reports. Minc-Golomb et al. (1996) demonstrated that cerebellar neurons express iNOS-IR and mRNA using fluorescent immunohistochemistry and in situ hybridization. Using RT-PCR, Jacobs (1997) demonstrated the presence of iNOS mRNA in the normal hypothalamus. Harada et al. (1999) reported that expression of iNOS mRNA by in situ hybridization is significantly induced after LPS stimulation in the paraventricular nucleus. Using immunohistochemistry and slot blots, Jacob et al. (1999) showed iNOS expression in normal facial motoneurons of adult rats.

The cellular distribution and intensity of expression of both ncNOS and iNOS are not equivalent at protein and mRNA levels in the spinal cord. For example, ncNOS-IR is absent in most large motoneurons even after Dyn spinal neurotoxicity, yet ncNOS hybridization data show more extensive distribution both in ncNOS-IR-negative as well as in ncNOS-IR-positive neurons. Similarly, iNOS-IR is present predominantly in glial and/or epithelial cells, but iNOS mRNA is expressed primarily in neurons as well as in glial cells. The reason for this discrepancy remains elusive. One possible explanation is the universal mRNA expression or existence in motoneurons. In the preliminary experiments, in situ hybridization was employed to measure expression of several genes including NOS, p75 nerve growth factor receptor, brain-derived neurotrophic factor, c-fos, and heat shock protein a and b. All these genes displayed various degrees of expression of iNOS in the spinal, facial and hypoglossal motoneurons. To confirm this observation, the reported genes were inspected for their expressions in the spinal and brain motoneurons with both radioactive and non-radioactive probes. The majority of the reported genes showed extensive mRNA expression in motoneurons with typical hybridization signals under both physiological and pathophysiological conditions (Hanemann et al., 1993; Ikeshima et al., 1993; Hammarberg et al., 1998; Jacobsson et al., 1998; Grossman et al., 1999; MacLennan et al., 1999; Nakagomi et al., 1999; Shibata et al., 1999). The universality of gene expression in motoneurons and its biological relevance remain to be elucidated. It appears that motoneurons express mRNA of many silent genes with reduced or no translation under normal constitutive conditions. These silent genes may be translated into proteins to meet an emergency under pathophysiological conditions.

Another possibility for the above variation might be the limited sensitivity and specificity of immunohistochemistry. The levels of NOS (antigen) in the (moto)neurons may be too low or too unstable to be detected by routine immunohistochemical techniques. Western blots of pure (moto)neuronal cultures might confirm the presence of NOS-IR in (moto)neurons. The currently available antibodies for iNOS are mostly produced against the isoform of iNOS in macrophages, which may be different from the isoform in the CNS. The available antibodies for ncNOS are derived from brain sources. Most, if not all, immunohistochemistry studies have not demonstrated expression of ncNOS-IR in most large motoneurons. Large motoneurons may have their own specific isoform of ncNOS.

In conclusion, using neurobehavioral tests, NOS bioassay, immunohistochemistry and in situ hybridization, the present study demonstrates that both ncNOS (mainly at early stages) and iNOS (at later stages) are involved in Dyn-induced SCI. Expression of ncNOS protein and mRNA is equivalent, and both increase as early as 30 min after Dyn-induced spinal neurotoxicity. These findings confirm a previous study employing NADPH-diaphorase histochemistry (Hu et al., 1996). iNOS mRNA expression is delayed but increases later at 2 h, iNOS activity and immunoreactivity increase at 4 h, and both persist for 24–48 h after intrathecal Dyn A(1–17) administration. In a concurrent experimental

study, pretreatment with the relatively selective inhibitors of both ncNOS and iNOS is neuroprotective, while nonselective inhibition of all isoforms of NOS aggravates Dyn spinal neurotoxicity (Hu et al., 1999). In addition, pretreatment with NO donor significantly prevents Dyn spinal neurotoxicity at lower doses, but at higher doses NO donor induces paralysis in normal rats (Hu et al., 1999). Taken together, the data provide strong evidence that NO/NOS plays an important role in the pathophysiological mechanisms of Dyn-induced SCI.

Acknowledgements

The research was supported by grants from the National Natural Science Foundation of China and China Medical Board of New York. We thank Dr Solomon H. Snyder, Dr Ted M. Dawson and Dr Charles J. Lowenstein for their generous gifts of NOS antibodies and cDNA plasmids. We also thank Dr W. S. Lynn and Dr E. Ryan for critical reading and helpful discussion.

References

Adamson, D.C., Wildemann, B., Sasaki, M., Glass, J.D., McArthur, J.C., Christov, V.I., Dawson, T.M., Dawson, V.L., 1996. Immunologic NO synthase: elevation in severe AIDS dementia and induction by HIV-1 gp41. Science 274 (5294), 1917–1921.

Behrens, M.I., Koh, J.Y., Muller, M.C., Choi, D.W., 1996. NADPH diaphorase-containing striatal or cortical neurons are resistant to apoptosis. Neurobiol. Dis. 3 (1), 72–75.

Behrmann, D.L., Bresnahan, J.C., Beattie, M.S., 1993. Comparison of YM-14673, U-50488H, and Nalmefene after spinal cord injury in the rat. Exp. Neurol. 587, 250–256.

Bethea, J.R., Castro, M., Keane, R.W., Lee, T.T., Dietrich, W.D., Yezierski, R.P., 1998. Traumatic spinal cord injury induces nuclear factor-kappaB activation. J. Neurosci. 18 (9), 3251–3260.

Bishop, A., Marquis, J.C., Cashman, N.R., Demple, B., 1999. Adaptive resistance to nitric oxide in motor neurons. Free Radic. Biol. Med. 26 (7–8), 978–986.

Bolanos, J.P., Almeida, A., 1999. Roles of nitric oxide in brain hypoxia-ischemia. Biochim. Biophys. Acta 1411 (2–3), 415–436.

Bredt, D.S., Snyder, S.H., 1990. Isolation of nitric oxide synthase, a calmodulin-requiring enzyme. Proc. Natl. Acad. Sci. USA 87 (2), 682–685.

Callsen-Cencic, P., Hoheisel, U., Kaske, A., Mense, S., Tenschert, S., 1999. The controversy about spinal neuronal nitric oxide synthase: under which conditions is it up- or downregulated? Cell Tissue Res. 295 (2), 183–194.

Catalan, R.E., Martinez, A.M., Aragones, M.D., Hernandez, F., 1996. Identification of nitric oxide synthases in isolated bovine brain vessels. Neurosci. Res. 25 (2), 195–199.

Chen, B., Tian, X.F., Jen, M.F., 1995. Dynorphin-induced spinal cord injury in rats. Chin. J. Pharmacol. Toxicol. 9, 36–39.

Coeroli, L., Renolleau, S., Arnaud, S., Plotkine, D., Cachin, N., Plotkine, M., Ben-Ari, Y., Charriaut-Marlangue, C., 1998. Nitric oxide production and perivascular tyrosine nitration following focal ischemia in neonatal rat. J. Neurochem. 70 (6), 2516–2525.

Dalkara, T., Moskowitz, M.A., 1994. The complex role of nitric oxide in the pathophysiology of focal cerebral ischemia. Brain Pathol. 4, 45–49.

Dubner, R., Ruda, M.A., 1992. Activity-dependent neuronal plasticity following tissue injury and inflammation. Trends Neurosci. 15 (3), 96–103.

Dumont, M., Lemaire, S., 1994. Dynorphin potentiation of [^{3}H]CGP-39653 binding to rat brain membranes. Eur. J. Pharmacol. 271, 241–244.

Dun, N.J., Dun, S.L., Wu, S.Y., Forstermann, U., Schmidt, H.H., Tseng, L.F., 1993. Nitric oxide synthase immunoreactivity in the rat, mouse, cat and squirrel monkey spinal cord. Neuroscience 54 (4), 845–857.

Endoh, M., Maiese, K., Pulsinelli, W.A., Wagner, J.A., 1993. Reactive astrocytes express NADPH diaphorase in vivo after transient ischemia. Neurosci. Lett. 154, 125–128.

Faden, A.I., 1990. Opioid and nonopioid mechanisms may contribute to dynorphins pathophysiological actions in spinal cord injury. Ann. Neurol. 27, 67–74.

Faden, A.I., Takemori, A.E., Pritoghese, P.S., 1987. Kappa-selective opiate antagonist norbinaltorphimine improves outcome after traumatic spinal cord injury in rats. CNS Trauma 4 (4), 227–237.

Grossman, S.D., Wolfe, B.B., Yasuda, R.P., Wrathall, J.R., 1999. Alterations in AMPA receptor subunit expression after experimental spinal cord contusion injury. J. Neurosci. 19 (14), 5711–5720.

Guizar-Sahagun, G., Garcia-Lopez, P., Espitia, A.L., Grijalva, I., Franco-Bourland, R.E., Madrazo, I., 1998. Transitory expression of NADPH diaphorase (NOS) in axonal swellings after spinal cord injury. Neuroreport 9 (12), 2899–2902.

Haas, J., Meyding-Lamade, U., Fath, A., Stingele, K., Storch-Hagenlocher, B., Wildemann, B., 1999. Acyclovir treatment of experimentally induced herpes simplex virus encephalitis: monitoring the changes in immunologic NO synthase expression and viral load within brain tissue of SJL mice. Neurosci. Lett. 264 (1–3), 129–132.

Hamada, Y., Ikata, T., Katoh, S., Tsuchiya, K., Niwa, M., Tsutsumishita, Y., Fukuzawa, K., 1996. Roles of nitric oxide in compression injury of rat spinal cord. Free. Radic. Biol. Med. 20 (1), 1–9.

Hammarberg, H., Risling, M., Hokfelt, T., Cullheim, S., Piehl, F., 1998. Expression of insulin-like growth factors and corresponding binding proteins (IGFBP 1-6) in rat spinal cord and peripheral nerve after axonal injuries. J. Comp. Neurol. 400 (1), 57–72.

Hanemann, C.O., Kuhn, G., Lie, A., Gillen, C., Bosse, F., Spreyer, P., Muller, H.W., 1993. Expression of decorin mRNA in the nervous system of rat. J. Histochem. Cytochem. 41 (9), 1383–1391.

Hassan, A.H., Pzewlocki, R., Herz, A., Stein, C., 1992. Dynorphin, a preferential ligand for kappa-opioid receptors, is present in nerve fibers and immune cells within inflamed tissue of the rat. Neurosci. Lett. 140 (1), 85–88.

Herz, A., 1996. Peripheral opioid analgesia — facts and mechanisms. Prog. Brain Res. 110, 95–104.

Higuchi, Y., Hattori, H., Hattori, R., Furusho, K., 1996. Increased neurons containing neuronal nitric oxide synthase in the brain of a hypoxic-ischemic neonatal rat model. Brain Dev. 18 (5), 369–375.

Hu, W.H., Lee, F.C.H., Wan, X.S.T., Chen, Y.T., Jen, M.F., 1996. Dynorhpin neurotoxicity induced nitric oxide synthase expression in ventral horn cells of rat spinal cord. Neurosci. Lett. 203, 13–16.

Hu, W.H., Zhang, C.H., Yang, H.F., Zheng, Y.F., Liu, N., Sun, X.J., Jen, J., Jen, M.F., 1998. The mechanism for dynorphin-induced dualistic effect on free intracellular Ca^{2+} concentration in cultured rat spinal neurons. Eur. J. Pharmacol. 342 (2–3), 325–332.

Hu, W.H., Li, F., Qiang, W.A., Liu, N., Wang, G.Q., Xiao, J., Liu, J.S., Liao, W.H., Jen, M.F., 1999. A dual role for nitric oxide in dynorphin spinal neurotoxicity. J. Neurotrauma 16 (1), 86–96.

Hylden, J.L., Nahin, R.L., Traub, R.J., Dubnerm, R., 1991. Effects of spinal kappa-opioid receptor agonists on the responsiveness of nociceptive superficial dorsal horn neurons. Pain 44 (2), 187–193.

Hyman, B.T., Marzloff, K., Wenniger, J.J., Dawson, T.M., Bredt, D.S., Snyder, S.H., 1992. Relative sparing of nitric oxide synthase-containing neurons in the hippocampal formation in Alzheimer's disease. Ann. Neurol. 32 (6), 818–820.

Iadecola, C., 1997. Bright and dark sides of nitric oxide in ischemic brain injury. Trends Neurosci. 20 (3), 132–139.

Iadecola, C., Xu, X., Zhang, F., El-Fakahany, E.E., Ross, M.E., 1995a. Marked induction of calcium-independent nitric oxide synthase activity after focal cerebral ischemia. J. Cereb. Blood Flow Metab. 15, 52–59.

Iadecola, C., Zhang, F., Xu, X., 1995b. Inhibition of inducible nitric oxide synthase ameliorates cerebral ischemic damage. Am. J. Physiol. 268, R286–R292.

Ikeshima, H., Yuasa, S., Matsuo, K., Kawamura, K., Hata, J., Takano, T., 1993. Expression of three nonallelic genes coding calmodulin exhibits similar localization on the central nervous system of adult rats. J. Neurosci. Res. 36 (1), 111–119.

Jacobsson, G., Piehl, F., Meister, B., 1998. VAMP-1 and VAMP-2 gene expression in rat spinal motoneurones: differential regulation after neuronal injury. Eur. J. Neurosci. 10 (1), 301–316.

Kaur, C., Singh, J., Moochhala, S., Lim, M.K., Lu, J., Ling, E.A., 1999. Induction of NADPH diaphorase/nitric oxide synthase in the spinal cord motor neurons of rats following a single and multiple non-penetrative blasts. Histol. Histopathol. 14 (2), 417–425.

Knerlich, F., Schilling, L., Gorlach, C., Wahl, M., Ehrenreich, H., Siren, A.L., 1999. Temporal profile of expression and cellular localization of inducible nitric oxide synthase, interleukin-1beta and interleukin converting enzyme after cryogenic lesion of the rat parietal cortex. Brain Res. Molec. Brain Res. 68 (1–2), 73–87.

Laughlin, T.M., Vanderah, T.W., Lashbrook, J., Nichols, M.L., Ossipov, M., Porreca, F., Wilcox, G.L., 1997. Spinally administered dynorphin A produces long-lasting allodynia: involvement of NMDA but not opioid receptors. Pain 72 (1–2), 253–260.

Lecanu, L., Verrecchia, C., Margaill, I., Boulu, R.G., Plotkine, M., 1998. iNOS contribution to the NMDA-induced excitotoxic lesion in the rat striatum. Br. J. Pharmacol. 125 (3), 584–590.

Li, F.C., Zuo, P.P., Hu, W.H., Liu, N., Jen, M.F., 1997. Glutamate involvement in rats with spinal cord injury induced by dynorphin A(1–17). Chin. J. Rehabil. Theory Practice 3, 6–9.

Li, Q., Eiden, L.E., Cavert, W., Reinhart, T.A., Rausch, D.M., Murray, E.A., Weihe, E., Haase, A.T., 1999. Increased expression of nitric oxide synthase and dendritic injury in simian immunodeficiency virus encephalitis. J. Hum. Virol. 2 (3), 139–145.

Licinio, J., Prolo, P., McCann, S.M., Wong, M.L., 1999. Brain iNOS: current understanding and clinical implications. Mol. Med. Today 5 (5), 225–232.

Liu, S., Adcock, I.M., Old, R.W., Barnes, P.J., Evans, T.W., 1993. Lipopolysaccharide treatment in vivo induces widespread tissue expression of inducible nitric oxide synthase mRNA. Biochem. Biophys. Res. Commun. 196, 1208–1213.

Long, J.B., Rigamonti, D.D., Oleshansky, M.A., Wingfield, C.P., Martinez-Arizala, A., 1994. Dynorphin A-induced rat spinal cord injury, evidence for excitatory amino acid involvement in a pharmacological model of ischemic spinal cord injury. J. Pharm. Exp. Therap. 269 (1), 358–366.

MacLennan, A.J., Devlin, B.K., Neitzel, K.L., McLaurin, D.L., Anderson, K.J., Lee, N., 1999. Regulation of ciliary neurotrophic factor receptor alpha in sciatic motor neurons following axotomy. Neuroscience 91 (4), 1401–1413.

Marsala, J., Kluchova, D., Marsala, M., 1997. Spinal cord gray matter layers rich in NADPH diaphorase-positive neurons are refractory to ischemia-reperfusion-induced injury: a histochemical and silver impregnation study in rabbit. Exp. Neurol. 145 (1), 165–179.

Mayer, B., John, M., Bohme, E., 1990. Purification of a Ca^{2+}/calmodulin-dependent nitric oxide synthase from porcine cerebellum. Cofactor-role of tetrahydrobiopterin. FEBS Lett. 277 (1,2), 215–219.

McCann, S.M., Licinio, J., Wong, M.L., Yu, W.H., Karanth, S., Rettorri, V., 1998. The nitric oxide hypothesis of aging. Exp. Gerontol. 33 (7–8), 813–826.

Meyding-Lamade, U., Haas, J., Lamade, W., Stingele, K., Kehm, R., Fath, A., Heinrich, K., Storch Hagenlocher, B., Wildemann, B., 1998. Herpes simplex virus encephalitis: long-term comparative study of viral load and the expression of immunologic nitric oxide synthase in mouse brain tissue. Neurosci. Lett. 244 (1), 9–12.

Molander, C., Xu, Q., Grant, G., 1984. The cytoarchitectonic organization of the spinal cord in the rat. I. The lower thoracic and lumbosacral cord. J. Comp. Neurol. 230 (1), 133–141.

Mufson, E.J., Brandabur, M.M., 1994. Sparing of NADPH-diaphorase striatal neurons in Parkinson's and Alzheimer's diseases. Neuroreport 5 (6), 705–708.

Murphy, S., Simmon, M.L., Agullo, L., Garcia, A., Feinstein, D.L., Galea, E., Reis, D.J., Minc-Golomb, D., Schwartz, J.P., 1993. Synthesis of nitric oxide in CNS glia cells. Trends Neurosci. 16, 323–328.

Nakagomi, S., Kiryu-Seo, S., Kimoto, M., Emson, P.C., Kiyama, H., 1999. Dimethylarginine dimethylaminohydrolase (DDAH) as a nerve-injury-associated molecule: mRNA localization in the rat brain and its coincident up-regulation with neuronal NO synthase (nNOS) in axotomized motoneurons. Eur. J. Neurosci. 11 (6), 2160–2166.

Parkinson, J.F., Mitrovic, B., Merrill, J.E., 1997. The role of nitric oxide in multiple sclerosis. J. Mol. Med. 75 (3), 174–186.

Perez-Severiano, F., Escalante, B., Rios, C., 1998. Nitric oxide synthase inhibition prevents acute quinolinate-induced striatal neurotoxicity. Neurochem. Res. 23 (10), 1297–1302.

Qiang, W.A., Liu, J., Lu, F.L., Liu, Z.Q., Liu, J.S., 1996. Measurement of NOS activity by monitoring the conversion of ^{3}H-arginine. Chin. J. Med. 76 (8), 567–571.

Rao, A.M., Dogan, A., Hatcher, J.F., Dempsey, R.J., 1998. Fluorometric assay of nitrite and nitrate in brain tissue after traumatic brain injury and cerebral ischemia. Brain Res. 793 (1–2), 265–270.

Salter, M., Knowles, R.G., Moncada, S., 1991. Widespread tissue distribution, species distribution and changes in activity of Ca^{2+}-dependent and Ca^{2+}-independent nitric oxide synthases. FEBS Lett. 291, 145–149.

Schmidt, W., Wolf, G., Calka, J., Schmidt, H.H.H.W., 1995. Evidence for bidirectional changes in nitric oxide synthase activity in the rat striatum after excitotoxically (quinolinic acid) induced degeneration. Neuroscience 67 (2), 345–356.

Seidel, B., Stanarius, A., Wolf, G., 1997. Differential expression of neuronal and endothelial nitric oxide synthase in blood vessels of the rat brain. Neurosci. Lett. 239 (2–3), 109–112.

Sheng, W.S., Hu, S., Gekker, G., Zhu, S., Peterson, P.K., Chao, C.C., 1997. Immunomodulatory role of opioids in the central nervous system. Arch. Immunol. Ther. Exp. (Warsz) 45 (5–6), 359–366.

Shibata, T., Watanabe, M., Ichikawa, R., Inoue, Y., Koyanagi, T., 1999. Different expressions of alpha-amino-3-hydroxy-5-methyl-4-isoxazole propionic acid and N-methyl-D-aspartate receptor subunit mRNAs between visceromotor and somatomotor neurons of the rat lumbosacral spinal cord. J. Comp. Neurol. 404 (2), 172–182.

Shukla, V.K., Lemaire, S., 1994. Non-opioid effect of dynorphins, possible role of the NMDA receptor. TiPS 15 (12), 420–424.

Skilling, S.R., Sun, X., Kurtz, H.J., Larson, A.A., 1992. Selective potentiation of NMDA-induced activity and release of excitatory amino acids by dynorphins: possible roles in paralysis and neurotoxicity. Brain Res. 575, 272–278.

Stojkovic, T., Colin, C., Le Saux, F., Jacque, C., 1998. Specific pattern of nitric oxide synthase expression in glial cells after hippocampal injury. Glia 22 (4), 329–337.

Strijbos, P.J., 1998. Nitric oxide in cerebral ischemic neurodegeneration and excitotoxicity. Crit. Rev. Neurobiol. 12 (3), 223–243.

Tachibana, T., Miki, K., Fukuoka, T., Arakawa, A., Taniguchi, M., Maruo, S., Noguchi, K., 1998. Dynorphin mRNA expression in dorsal horn neurons after traumatic spinal cord injury: temporal and spatial analysis using in situ hybridization. J. Neurotrauma 15 (7), 485–494.

Takeuchi, A., Isobe, K.I., Miyaishi, O., Sawada, M., Fan, Z.H., Nakashima, I., Kiuchi, K., 1998. Microglial NO induces delayed neuronal death following acute injury in the striatum. Eur. J. Neurosci. 10 (5), 1613–1620.

Tian, X.F., Chen, B., Jen, M.F., 1994. The study on the mechanisms underlying dynorphin spinal neurotoxicity. Chin. J. Physiol. Sci. 10, 289–297.

Van Dam, A.M., Bauer, J., Man-A-Hing, W.K.H., Marquette, C., Tilders, F.J.H., Berkenbosch, F., 1995. Appearance of inducible nitric oxide synthase in the rat central nervous system after rabies virus infection sand during experimental allergic encephalomyelitis but not after peripheral administration of endotoxin. J. Neurosci. Res. 40, 251–260.

Vizzard, M.A., 1997. Increased expression of neuronal nitric oxide synthase in bladder afferent and spinal neurons following spinal cord injury. Dev. Neurosci. 19 (3), 232–246.

Vizzard, M.A., Erdman, S.L., Erickson, V.L., Stewart, R.J., Roppolo, J.R., De Groat, W.C., 1994. Localization of NADPH diaphorase in the lumbosacral spinal cord and dorsal root ganglia of the cat. J. Comp. Neurol. 339 (1), 62–75.

Wada, K., Chatzipanteli, K., Kraydieh, S., Busto, R., Dietrich, W.D., 1998. Inducible nitric oxide synthase expression after traumatic brain injury and neuroprotection with aminoguanidine treatment in rats. Neurosurgery 43 (6), 1427–1436.

Wada, K., Chatzipanteli, K., Busto, R., Dietrich, W.D., 1999. Effects of L-NAME and 7-NI on NOS catalytic activity and behavioral outcome after traumatic brain injury in the rat. J. Neurotrauma 16 (3), 203–212.

Wallace, M.N., Fredens, K., 1992. Activated astrocytes of the mouse hippocampus contain high levels of NADPH-diaphorase. NeuroReport 3, 953–956.

Winkler, T., Sharma, H.S., Stalberg, E., Badgaiyan, R.D., Alm, P., Westman, J., 1998. Spinal cord evoked potentials and edema in the pathophysiology of rat spinal cord injury. Involvement of nitric oxide. Amino Acids 14 (1–3), 131–139.

Wu, W., Liuzzi, F.J., Depto, A.S., Li, Y., Mong, J.A., Dawson, T.M., Snyder, S.H., 1994. Neuronal nitric oxide synthase is induced in spinal neurons by traumatic injury. Neuroscience 61, 719–726.

Xu, M., Ng, Y.K., Leong, S.K., 1998. Induction of microglial reaction and expression of nitric oxide synthase I in the nucleus dorsalis and red nucleus following lower thoracic spinal cord hemisection. Brain Res. 808 (1), 23–30.

Yaksh, T.L., Rudy, T.A., 1976. Chronic catheterization of the spinal sub-arachnoid space. Physiol. Behav. 17, 1031–1036.

Yamanaka, K., Kumura, E., Yoshimine, T., Maruno, M., Taniguchi, M., Kosaka, H., Hayakawa, T., 1998. Cellular expression of inducible nitric oxide synthase following rat cortical incision and its suppression by hydroxyl radical scavenger, 1,2-is(nicotinamido)propane. Neurosci. Res. 31 (4), 347–350.

Zhang, Z.G., Chopp, M., Gautam, S., Zaloga, C., Zhang, R.L., Schmidt, H.H.H.W., Pollock, J.S., Forstermann, U., 1994. Upregulation of neuronal nitric oxide synthase and mRNA, and selective sparing of nitric oxide synthase-containing neurons after focal cerebral ischemia in rat. Brain Res. 654, 85–95.

Zhang, F., Casey, R., Ross, M.E., Iadecola, C., 1996. Aminoguanidine ameliorates and L-arginine worsens brain damage from intraluminal middle cerebral artery occlusion. Stroke 27, 317–323.